From neurons to circuits: linear estimation of local field potentials

M. Rasch, N.K. Logothetis, G. Kreiman

Supplementary Material

---

1. Supplementary Methods

1.1 Relationship between mean squared error and correlation

Let the LFP ($L(t)$) and its estimate ($L_{est}(t)$) both have a mean of zero and a variance of 1. The mean squared error between the and its estimate is defined by:

$$\varepsilon^2 = < (L(t) - L_{est}(t))^2 >$$

where <> denote the mean over the entire recording trial.

The Pearson correlation coefficient between $L(t)$ and $L_{est}(t)$ is defined by:

$$r = \frac{< L(t)L_{est}(t) > - < L(t) >< L_{est}(t) >}{\sqrt{< (L(t) - < L(t) >)^2 >}\sqrt{< (L_{est}(t) - < L_{est}(t) >)^2 >}}$$

Throughout the text, we subtract the mean and set the standard deviation to 1 ($< L(t) >=< L_{est}(t) >= 0$ and $< (L(t) - < L(t) >)^2 >=< (L_{est}(t) - < L_{est}(t) >)^2 >= 1$). Therefore, we have:

$$\varepsilon^2 = 2(1 - r)$$

This relationship between r and ε^2 is illustrated for the actual data in **Figure S1F**. Throughout the text, we report r and we refer to this measure of how close $L_{est}(t)$ is to $L(t)$ as the "estimation accuracy".

1.2 Derivation of the general W-K filter (h_{mean})

We consider a situation where we have N recordings. These N recordings could come from N separate trials for the same electrode or from N different electrodes. In each of these recordings, we have a spike train, $x_j(t)$, and the corresponding LFP, $L_j(t)$. The signals are normalized so that they have zero mean

and a standard deviation of 1. We aim to find a filter that minimizes the sum of the mean squared errors in the LFP estimations:

$$\varepsilon^2 = \frac{1}{N}\sum_{j=1}^{N}\int dt\left[L_j(t) - \int h(t-\tau)x_j(\tau)d\tau\right]^2$$

Rewriting $L_j(t)$, h and $x_j(t)$ in terms of their Fourier transforms ($\hat{L}_j$, $\hat{h}$ and $\hat{x}_j$), the expression in the square bracket can be written as:

$$\left[\int dk e^{ikt}\hat{L}_j(k) - \int d\tau \int dk' \int dk'' e^{ik'(t-\tau)}e^{ik''\tau}\hat{h}(k')\hat{x}_j(k'')\right]\cdot\left[\int dp e^{ipt}\hat{L}_j(p) - \int d\tau' \int dp' \int dp'' e^{ip'(t-\tau')}e^{ip''\tau'}\hat{h}(p')\hat{x}_j(p'')\right]$$

This can in turn be expanded into:

$$\int dk \int dp e^{i(k+p)t}\hat{L}_j(k)\hat{L}_j(p) - \int d\tau \int dk' \int dk'' \int dp e^{ik'(t-\tau)}e^{ik''\tau}e^{ipt}\hat{h}(k')\hat{x}_j(k'')\hat{L}_j(p) -$$

$$-\int d\tau' \int dp' \int dp'' \int dk e^{ikt}e^{ip'(t-\tau')}e^{ip''\tau'}\hat{h}(p')\hat{x}_j(p'')\hat{L}_j(k) +$$

$$+\int d\tau \int d\tau' \int dk' \int dk'' \int dp' \int dp'' e^{ik'(t-\tau)}e^{ik''\tau}e^{ip'(t-\tau')}e^{ip''\tau'}\hat{h}(p')\hat{x}_j(p'')\hat{h}(k')\hat{x}_j(k'')$$

Solving the integrals in t, τ and τ' and simplifying, we obtain:

$$\varepsilon^2 = \frac{1}{2\pi N}\sum_{j=1}^{N}\int dk\left(\hat{L}_j(k) - \hat{h}(k)\hat{x}_j(k)\right)\left(\hat{L}_j(k) - \hat{h}(k)\hat{x}_j(k)\right)^* = \frac{1}{2\pi N}\int dk\,\eta(k)$$

where

$$\eta(k) = \sum_{j=1}^{N}\left|\hat{L}_j(k) - \hat{h}(k)\hat{x}_j(k)\right|^2$$

To find the optimal filter, we minimize ε^2, which is equivalent to minimizing η:

$$\frac{d\eta}{dh} = \frac{d}{dh}\left[\sum_{j=1}^{N}\left|\hat{L}_j(k) - \hat{h}(k)\hat{x}_j(k)\right|^2\right] = \sum_{j=1}^{N}\frac{d}{dh}\left[(\hat{L}_j - \hat{h}\hat{x}_j)(\hat{L}_j - \hat{h}\hat{x}_j)^*\right]$$

Setting the derivative to 0 and simplifying, we obtain:

$$\hat{h}(k) = \frac{\sum_{j=1}^{N}\hat{x}_j^*\hat{L}_j}{\sum_{j=1}^{N}\hat{x}_j^*\hat{x}_j} = \frac{\sum_{j=1}^{N}\Phi_{Lx}(k)}{\sum_{j=1}^{N}\Phi_{xx}(k)}$$

where Φ_{Lx} is the cross-power spectrum between the LFP and the spike train and Φ_{xx} is the power spectrum of the spike train. This corresponds to Eq. 8 in the main text.

1.3 Relationship between the spike-LFP coherence and the mean squared error

For a single spike train, the optimum linear estimator is given by:

$$\hat{h}(k) = \frac{\Phi_{Lx}(k)}{\Phi_{xx}(k)}$$

and the mean squared error between the LFP and its estimate can be written as:

$$\varepsilon^2 = \frac{1}{2\pi} \int dk \left| \hat{L}_j(k) - \hat{h}(k)\hat{x}_j(k) \right|^2$$

Several investigators in the field have used the coherence between the spike train and the LFP, C, defined as:

$$C(k) = \frac{\Phi_{Lx}(k)}{\sqrt{\Phi_{xx}(k)\Phi_{LL}(k)}}$$

We can rewrite ε^2 in terms of the coherence:

$$\varepsilon^2 = \frac{1}{2\pi} \int dk \left[1 - \left| C(k) \right|^2 \right] \Phi_{LL}(k)$$

The coherence, weighted by the power spectrum of the LFP determines the minimum error in the linear estimation of the LFP.

Supplementary Figures Legends

Figure S1: LFP and spike train power spectral densities

(**A**) Normalized LFP power spectral density of 3 example electrodes in V1 from one monkey during spontaneous activity. Here we show the power spectral density, in log-log scale, averaged across 5 "trials" after normalization by the maximum. The dashed line is a linear fit, *s* indicates the slope for the linear fit.

(**B**) Normalized spike train power spectral density of the same 3 example electrodes shown in part **A**. The three spike trains correspond to multi-unit activity.

(**C**) Average normalized LFP power spectral density for all the electrodes and trials recorded from one monkey (including the 3 electrodes shown in part **A**). Error bars indicate one SEM (n=35). The dashed line is a linear fit, the *s* value is the slope.

(**D**) Average normalized spike train power spectral density for all the electrodes and trials recorded from the same monkey in part (**C**).

(**E**) Disitibution of linear fit slopes computed as indicated in part **A** for all the trials and electrodes. Bin size = 0.1. The arrow indicates the mean of the distribution.

(**F**) Relationship between the summed squared error (ε^2) and the correlation coefficient between $L(t)$ and $L_{est}(t)$ for all the electrodes in part **E** (n=109). Under the assumptions in the text ($\langle L(t)\rangle=\langle L_{est}(t)\rangle=0$ and $var[L(t)]=var[L_{est}(t)]=1$), there is a simple linear relationship between these two metrics comparing the LFP and its estimate (see 1.1).

Figure S2: Dependence on nfft and distribution of estimation accuracies

(**A**) Dependence of the estimation accuracy on the number of points used to compute the convolutions and Fourier transforms (nfft). The gray bars indicate the estimation accuracies while the black squares indicate the reconstruction accuracies. The reconstruction accuracies use the same data segment to estimate the W-K filter and to estimate the LFP whereas the estimation accuracies use separate data. Throughout the text, all the figures, analyses and conclusions are based on the estimation accuracies computed using nfft=2048 (arrow). The black triangles indicate the estimation accuracies obtained under the null hypothesis (using spike trains with the same firing rates as the experimental spike trains but with random Poisson statistics, see Methods).

(**B**) Estimation accuracy (r) distribution based on single trials ("trial-specific" W-K filters) for all V1 electrodes during spontaneous activity. The black arrow indicates the mean of the distribution. The gray curve shows the distribution of the reconstruction accuracy values (using the same spike/LFP data to compute the W-K filter and to compute the estimate; see Methods); the black arrow shows the mean of the estimation accuracies and the gray arrow shows the mean of the reconstruction accuracies. The dashed line shows the mean estimation accuracy under the null hypothesis (generating a Poisson spike train with the same number of spikes as the experimental spike trains) and the dotted lines show the range of the estimation accuracies under the null hypothesis.

Figure S3: Example LFP estimates

Examples of LFP recordings and LFP estimates from two different electrodes in two monkeys (spontaneous activity, V1). The format is the same as in **Figure 2** in the main text. The electrode shown in **B** is the same one shown in **Figure 2A** in the main text. For each electrode, here we show 6 different 1-second samples. The interval of 1 second is used here for illustration purposes only and is not used in any of the computations. The 6 segments are shown in the actual occurrence order but they are not consecutive. For each sample, we indicate the number of spikes (n) to illustrate the variability in spike counts across different 1-second samples. The solid line indicates the LFP recording and the dashed line shows the LFP estimate (see scale bar below the last segment). The "electrode-specific" W-K filters are shown at the bottom of the figure. We show the filter only for time lags between -800 and +800 ms (the actual number of points in the filter was $nfft$+1 where $nfft$=2048).

Figure S4: Correlation between estimation accuracy and firing rate, CV, and LFP power

(**A**) For each electrode recorded in V1 during spontaneous activity (n=109) we show the "trial-specific" estimation accuracy (average across all trials) as a function of the firing rate (computed over the entire trial and averaged across all trials). The dashed line shows a linear fit (correlation coefficient = 0.49).

(**B**) For each electrode, the estimation accuracy is shown as a function of the total power of the normalized LFP. The format is the same as in part **A** (correlation coefficient = 0.44).

(**C**) For each spike train, we computed the coefficient of variation of the interspike interval distribution (CV). Note that many of these values are >1 because the spike train comes from multiple-unit activity (MUA). The format is the same as in part **A** (correlation coefficient = 0.59).

(**D-F**) Correlation between estimation accuracy and firing rate (**D**), normalized LFP power (**E**) and interspike interval coefficient of variation (**F**) for individual trials. The format is the same as in part **A** except for the lack of averaging across trials.

Figure S5: Correlation between estimation accuracy for spontaneous activity and stimulus-driven activity

There was a strong correlation between the estimation accuracy (r) computed during spontaneous activity (x-axis) and the estimation accuracy computed during stimulus-driven activity (y-axis). The gray dashed line shows the linear fit ($n=71$ electrodes; correlation coefficient $\rho=0.64$).

Figure S6: LFP estimations from nearby LFP recordings

(**A**) We estimated the LFP time course from LFPs recorded from nearby electrodes using the same procedure described in Eqs. 2-4 to estimate the LFP from spike trains. Here we show a 1 second sample of an LFP recording ($L(t)$, solid line) and its estimate ($L_{est}(t)$, dashed line) using the LFP recorded from a separate electrode located 1 mm away.

(**B**) W-K filter for the example LFP estimation in part **A**.

(**C**) Using the same approach used when estimating LFPs from spike trains, we measured the accuracy in the estimation by computing the correlation coefficient between the LFP and its estimate. Here we show the average estimation accuracy (r) as a function of the distance between electrodes (bin size = 1 mm). The error bars denote one SEM. The squares indicate the average reconstruction accuracies (using the same data to compute the W-K filter and to estimate the LFP).

Figure S7: LFP estimation using the spike-triggered average

(**A**) Average "electrode-specific" spike-triggered average (STA) of the LFP over all the electrodes recorded in V1 (spontaneous activity, n=88 electrodes).

(**B**) Average "electrode-specific" W-K filter over all the electrodes recorded in V1 (spontaneous activity, n=88 electrodes).

(**C**) Estimation accuracy (r) using the W-K filter (gray) or the spike-triggered-average (STA) of the LFP (black). The estimation accuracies were averaged for all electrodes in each monkey. Error bars indicate one SEM. The squares indicate the reconstruction accuracies. The triangles indicate the estimation accuracies obtained under the null hypothesis.

Figure S8: Estimating the LFP in the LGN

(**A**) Example showing one second of an LFP recording in the LGN during spontaneous activity (solid line) and its estimation (dashed line). The estimation accuracy was 0.01.

(**B**) W-K filter for the electrode shown in part **A** (compare with the typical W-K filters shown in **Figures 2-4**).

(**C**) Estimation accuracy for all the electrodes in the LGN in 2 monkeys (spontaneous activity). The bars indicate the "electrode-specific" estimation accuracies (see Methods). The squares show the reconstruction accuracies (using the same data to compute the W-K filter and to estimate the LFP) and the triangles indicate the estimation accuracies under the null hypothesis (Poisson spike trains with the same spike counts). Only one of the electrodes showed statistically significant estimation accuracy (p<0.01, two-tailed t-test comparing against the null hypothesis) but even for this electrode, the estimation accuracy was quite poor compared with the values reported for V1 (cf. Figure S2**B**).

Figure S9: Single unit activity versus multi-unit activity

(**A**) Dependence of the estimation accuracy on the spike quality threshold for recordings during visual stimulation in V1. The "quality threshold" refers to the number of standard deviations above the high-pass filtered extracellular signal noise used as a threshold to determine the MUA spike occurrence times. The format and conventions are the same as the ones in **Figure 3**; squares indicate the reconstruction accuracy and the triangles

indicate performance under the null hypothesis (n=88 electrodes). The weak decrease in estimation accuracy with quality threshold is due to the decrease in the total number of spikes. The dashed line indicates the estimation accuracy obtained upon normalizing the number of spikes across all threshold values by randomly subsampling the spike trains. The values reported throughout the text correspond to a quality threshold of 5. (**B**) The waveforms surrounding the thresholded high-pass filtered extracellular signals (3 ms around the action potential peak) were used as input to a spike sorting algorithm (Quian Quiroga et al 2004). This algorithm separates the spike waveforms into clusters and assigns these clusters to multi-units (MUA) or single-units (SUA). Here we show the estimation accuracy using all the spikes from those electrodes that contained single-unit clusters (labeled "ALL(SUA)"), using all the spikes from those electrodes that contained multi-unit clusters (labeled "ALL(MUA)"), from the single-unit spikes ("SUA") and from the multi-unit spikes ("MUA"). The conventions are the same as in part (**A**). (**C**) Wiener-Kolmogorov filters for the MUA (light gray) and for the SUA (dark gray). The W-K filters shown here correspond to the average over 13 electrodes (SUA) and 21 electrodes (MUA).

Figure S1

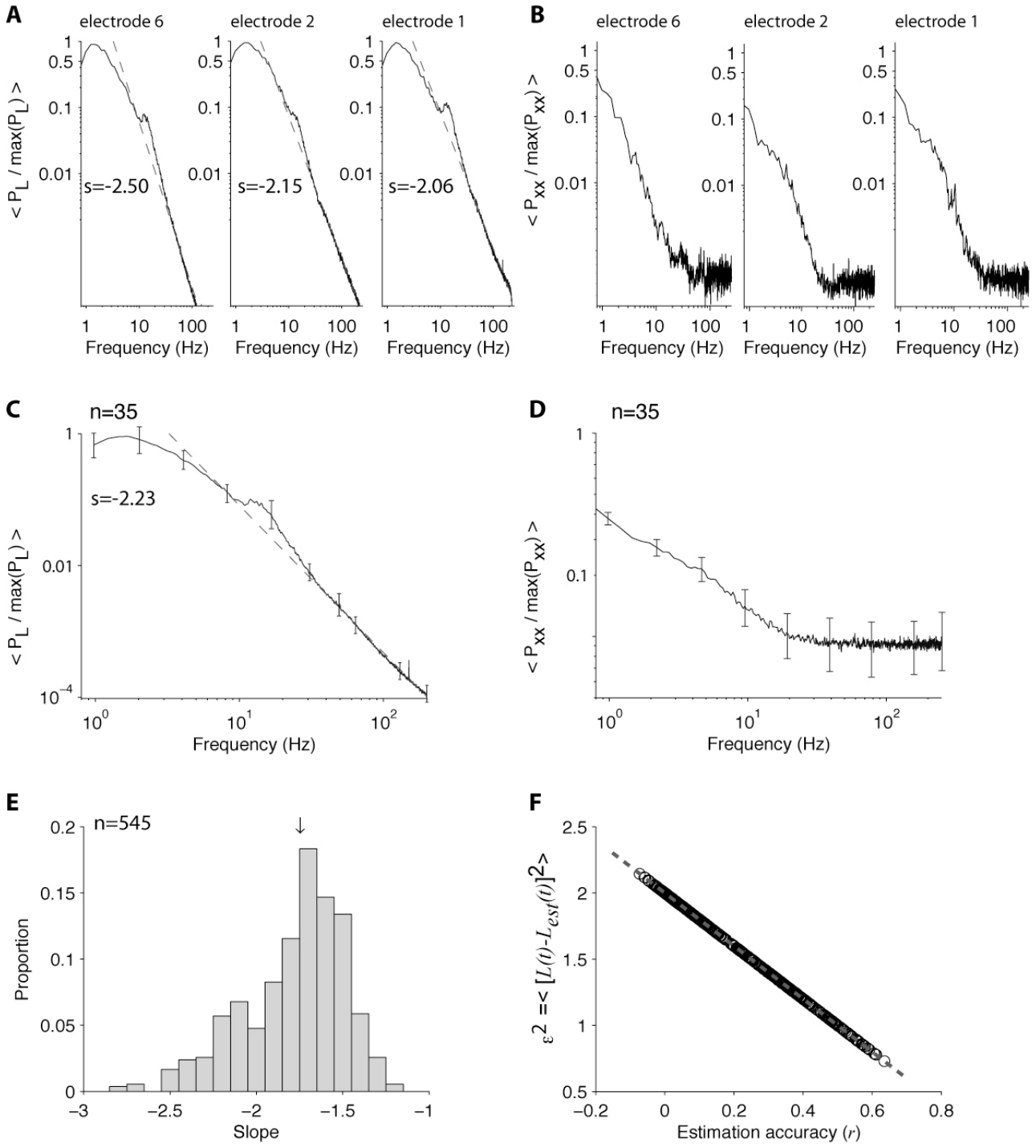
A
electrode 6
electrode 2
electrode 1
< P_L / max(P_L) >
s=-2.50
s=-2.15
s=-2.06
Frequency (Hz)
B
< P_xx / max(P_xx) >
C
n=35
s=-2.23
D
E
n=545
Proportion
Slope
F
ε2 =< [L(t)-L_est(t)]2>
Estimation accuracy (r)

Figure S2

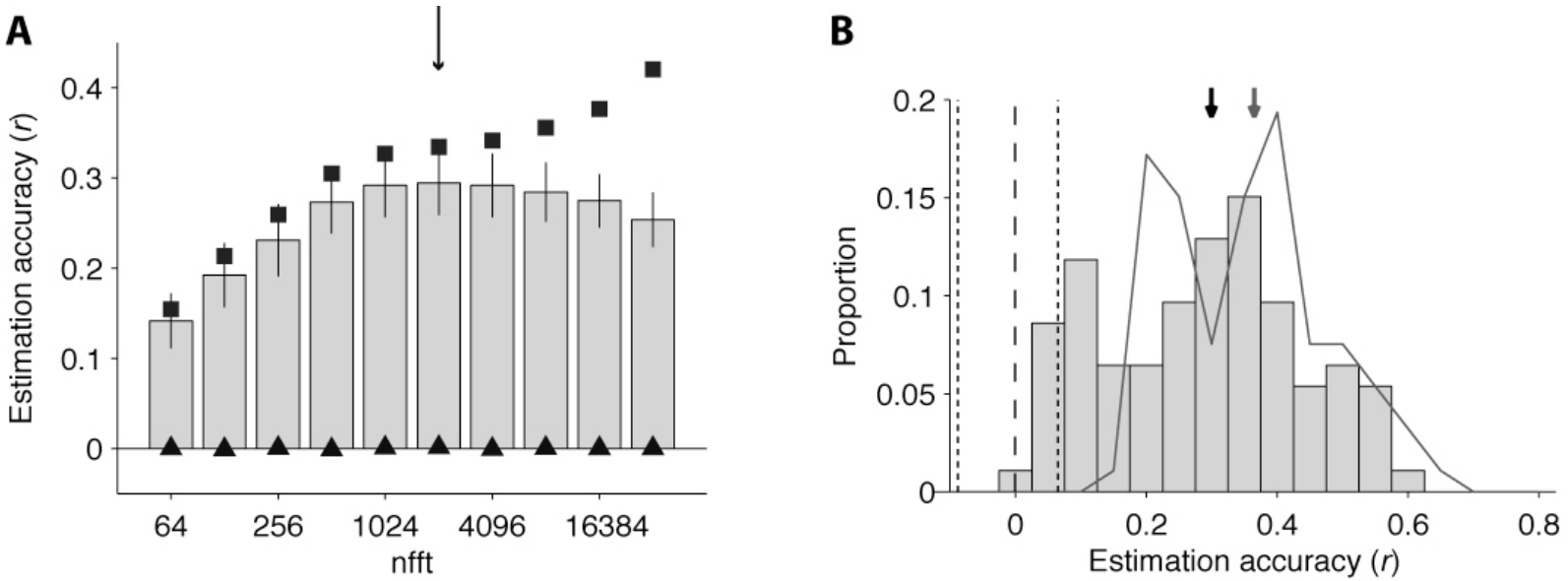
A
Estimation accuracy (r)
0.4
0.3
0.2
0.1
0
64
256
1024
4096
16384
nfft
B
Proportion
0.2
0.15
0.1
0.05
0
0
0.2
0.4
0.6
0.8
Estimation accuracy (r)

Figure S3

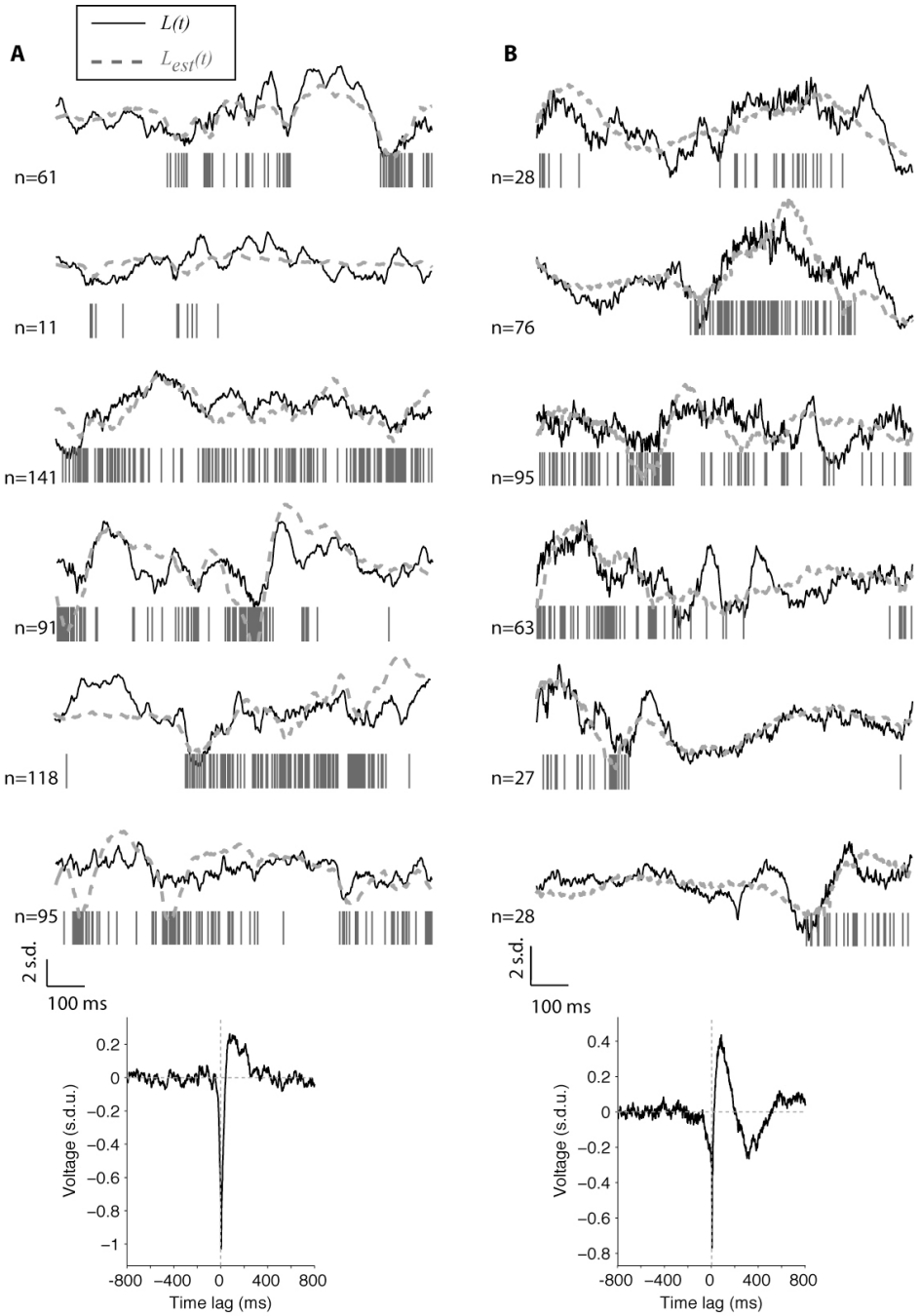
A
B
L(t)
$L_{est}(t)$
n=61
n=11
n=141
n=91
n=118
n=95
n=28
n=76
n=95
n=63
n=27
n=28
2 s.d.
100 ms
Voltage (s.d.u.)
Time lag (ms)
-800
-400
0
400
800

Figure S4

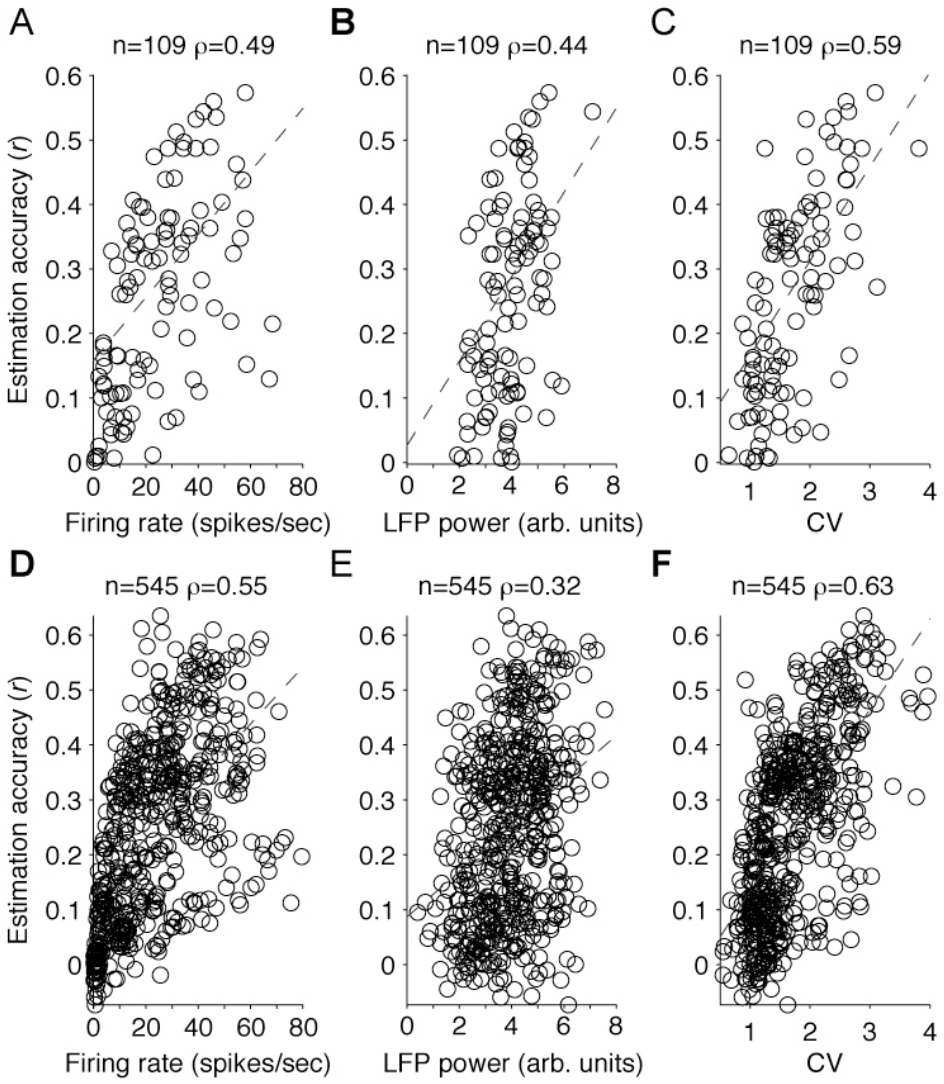
A
n=109 ρ=0.49
B
n=109 ρ=0.44
C
n=109 ρ=0.59
D
n=545 ρ=0.55
E
n=545 ρ=0.32
F
n=545 ρ=0.63
Estimation accuracy (r)
Firing rate (spikes/sec)
LFP power (arb. units)
CV

Figure S5

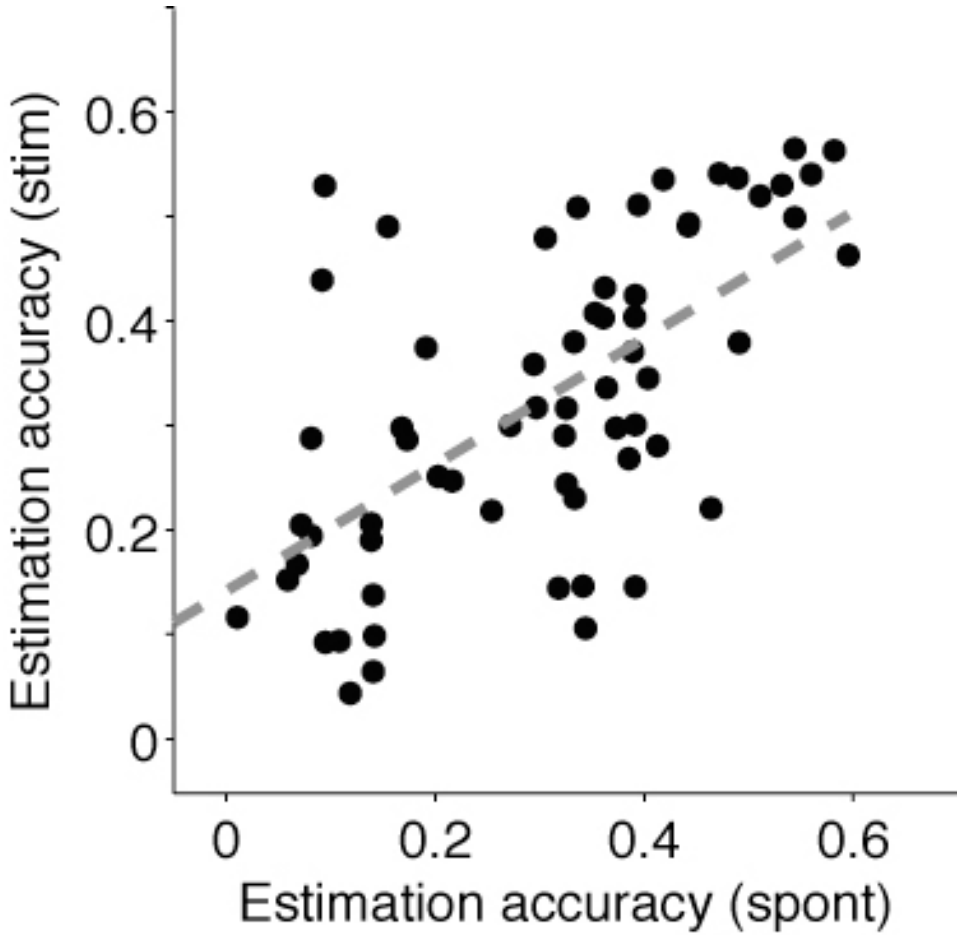
Estimation accuracy (stim)
0.6
0.4
0.2
0
0
0.2
0.4
0.6
Estimation accuracy (spont)

Figure S6

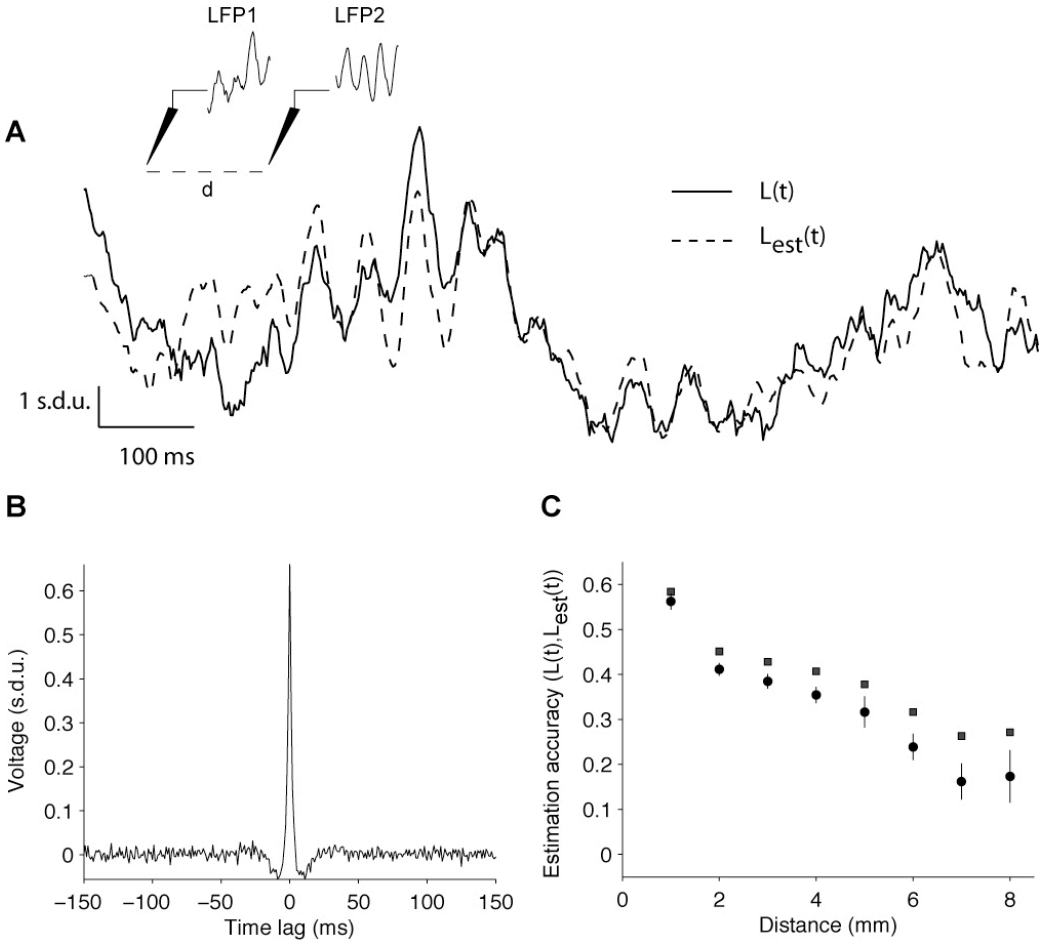
A
LFP1
LFP2
d
L(t)
$L_{est}(t)$
1 s.d.u.
100 ms
B
Voltage (s.d.u.)
0.6
0.5
0.4
0.3
0.2
0.1
0
−150 −100 −50 0 50 100 150
Time lag (ms)
C
Estimation accuracy ($L(t), L_{est}(t)$)
0.6
0.5
0.4
0.3
0.2
0.1
0
0 2 4 6 8
Distance (mm)

Figure S7

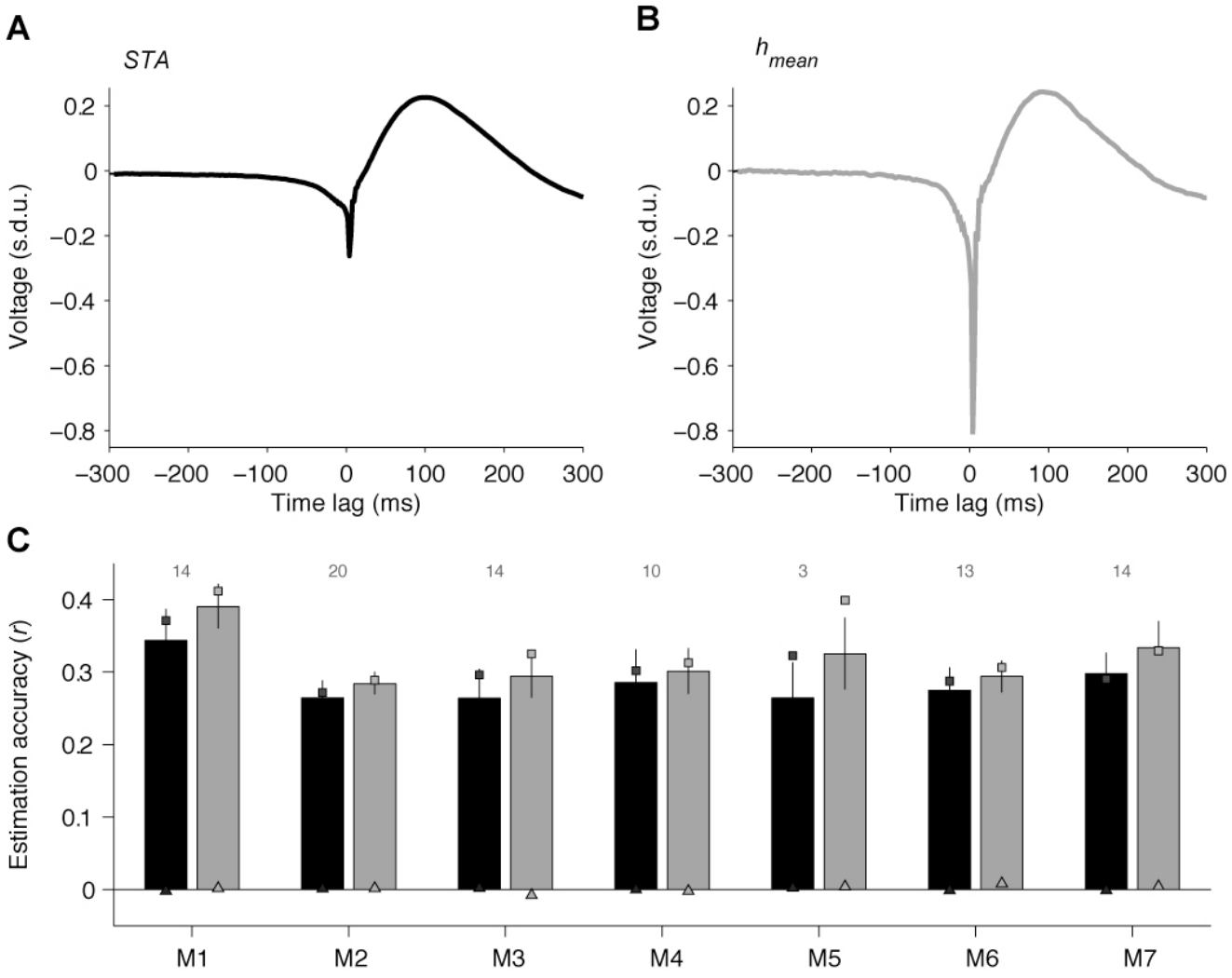
A
STA
Voltage (s.d.u.)
0.2
0
−0.2
−0.4
−0.6
−0.8
−300 −200 −100 0 100 200 300
Time lag (ms)
B
h_{mean}
Voltage (s.d.u.)
0.2
0
−0.2
−0.4
−0.6
−0.8
−300 −200 −100 0 100 200 300
Time lag (ms)
C
14 20 14 10 3 13 14
Estimation accuracy (r)
0.4
0.3
0.2
0.1
0
M1 M2 M3 M4 M5 M6 M7

Figure S8

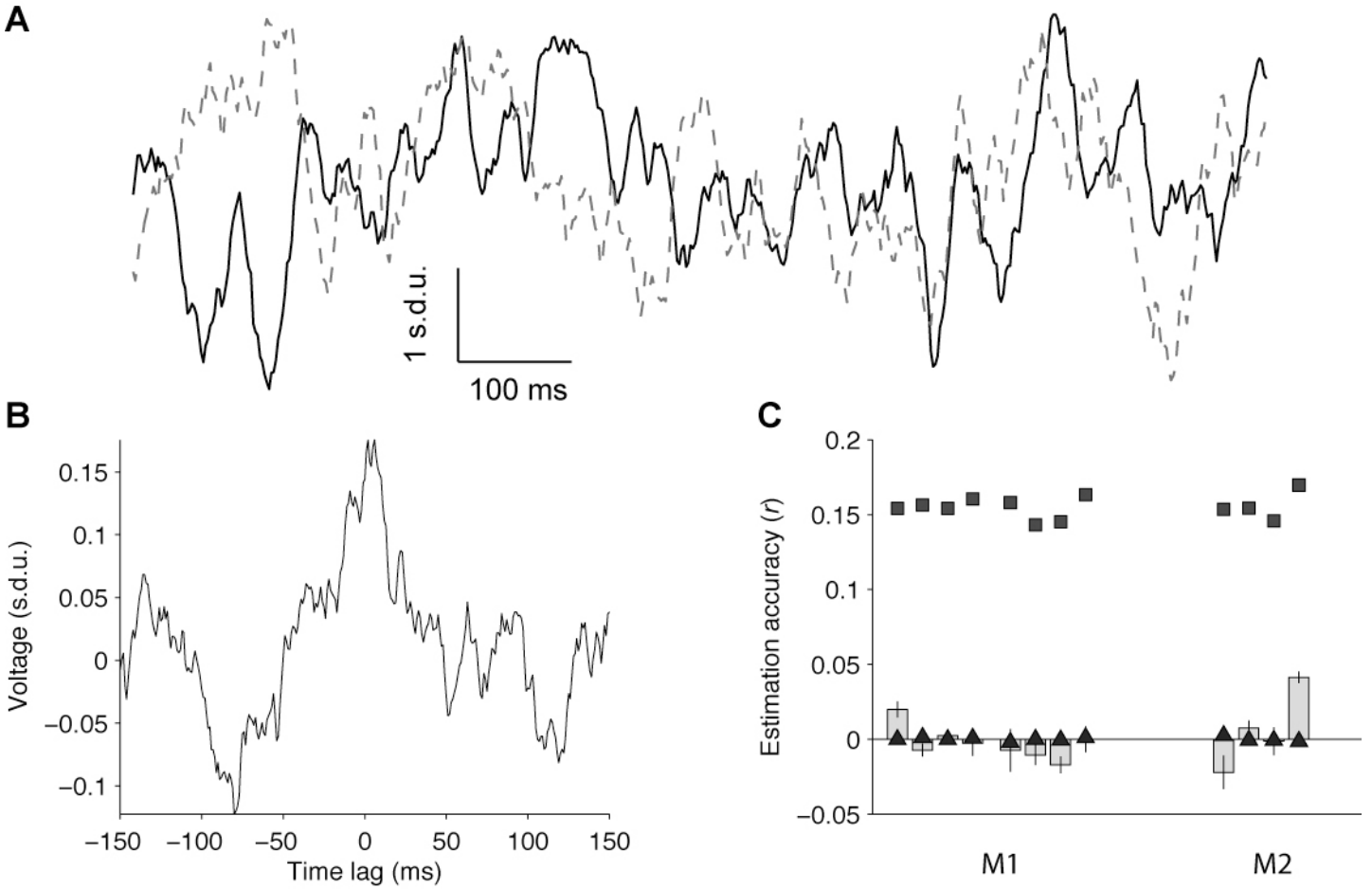
A
1 s.d.u.
100 ms
B
Voltage (s.d.u.)
0.15
0.1
0.05
0
−0.05
−0.1
−150
−100
−50
0
50
100
150
Time lag (ms)
C
Estimation accuracy (r)
0.2
0.15
0.1
0.05
0
−0.05
M1
M2

Figure S9

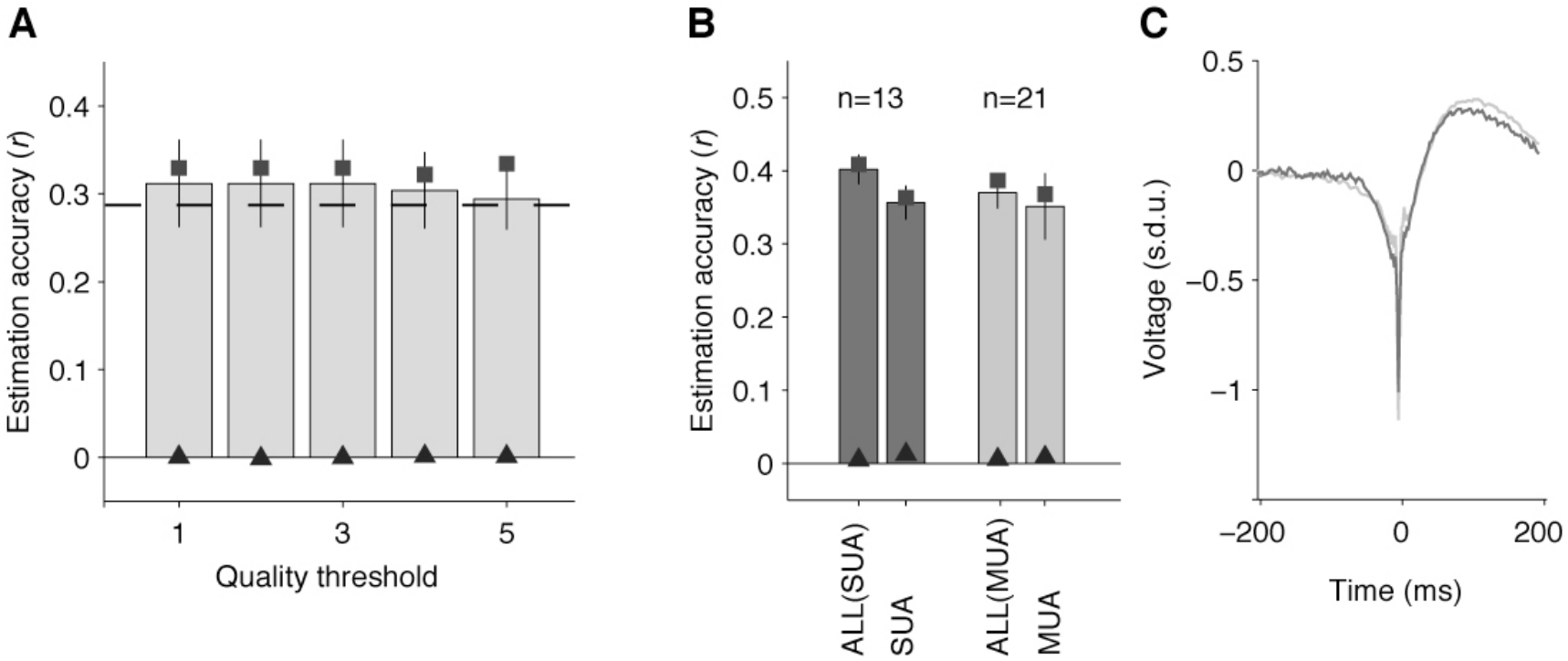
A
Estimation accuracy (r)
0.4
0.3
0.2
0.1
0
1
3
5
Quality threshold
B
Estimation accuracy (r)
0.5
0.4
0.3
0.2
0.1
0
n=13
n=21
ALL(SUA)
SUA
ALL(MUA)
MUA
C
Voltage (s.d.u.)
0.5
0
−0.5
−1
−200
0
200
Time (ms)